

Instanton Bags, High Density Holographic QCD and Chiral Symmetry Restoration

S. Bolognesi

*Department of Physics E. Fermi and INFN, University of Pisa
Largo Pontecorvo, 3, Ed. C, 56127 Pisa, Italy*

and

*Department of Mathematical Sciences,
Durham University, Durham DH1 3LE, U.K.*

Email: stefanobolo@gmail.com

May 2014

Abstract

We describe the simplest example of an instanton bag in Euclidean space. It consists of a monopole wall and a Kaluza-Klein monopole wall, lifted to one higher dimension, trapping the instanton charge in the middle. This object has finite instanton density in a three-dimensional volume.

Baryon physics in holographic QCD models gets translated into a multi-instanton problem in the bulk, and a state with a high density baryonic charge consists of a non-diluted multi-instanton solution. The instanton bag is a good candidate for this high-density state. We compute its parameters via moduli stabilization. Chiral symmetry restoration is exhibited by this state, and it is a direct consequence of its non-diluted features.

1 Introduction

Holographic QCD (HQCD) has been the subject of intense studies because it provides an environment to address strong coupling QCD questions with the use of semi-classical computations. Baryons of the QCD-like theory defined on the boundary correspond to instantons in the bulk. Thus, having a finite baryonic density in the dual theory corresponds to having a finite density of instantons in the bulk. The problem of the high-density phase of QCD is thus translated into a multi-instanton problem, which, even at the classical level, remains quite a difficult challenge, both numerically and analytically. Recently with P. Sutcliffe, we considered a toy model in $2 + 1$ dimension in which the high-density phase can be studied both analytically and numerically [1]. This model showed that the dilute approximation breaks down, as expected, exactly at the densities when the solitons are sufficiently close to start to populate the holographic direction.

Solitons are not hard objects but can compenetrate with one another. A high-density phase of solitons may be in the form of a collective structure, which is completely different from a coarse-grained version of a large number of small constituents. This phenomenon has been observed both for vortices and monopoles [2] and is known as ‘solitonic bag’. We still do not have a proper soliton bag description for multi-instanton configurations, although it has been suggested that this should somehow exist [3,4]. One obstacle in finding such a solution for instantons is that for the Yang-Mills theory in Euclidean space, instantons do not have an intrinsic scale. Thus, it is not uniquely defined how to make a high-density limit of instantons; the sizes must be specified in the limiting process. HQCD is a situation in which instantons do have an intrinsic scale. This scale is fixed by a balance between the curvature of the background geometry and the Chern-Simons coupling, which makes the instanton electrically charged. We may expect that a large number of instantons in HQCD could form a bag structure at large enough density.

QCD at high-density is expected to exhibit a phase transition in which chiral symmetry is restored. Moreover, there is a competition between two other possible instabilities: color superconductivity and chiral density waves. The second one is favored in the large N_c limit [5, 6]. Holographic models of QCD, being particular cases of large N_c QCD-type models, are thus expected to have chiral symmetry restoration together with chiral waves. Recently, these questions have been addressed in HQCD [7], where it has been found that, using an instanton fluid approximation, there is no sign of those phases. We will show that they are instead realized in the instanton bag background. Another generic expectation from large N_c QCD is the existence of a ‘quarkyonic phase’ [8]. This is generally believed to correspond, in HQCD, to the instantons populating the holographic direction [7,9,10], so that many instantons share the same 3D spatial section. Yet a different phase in HQCD has been discussed in [11,12] and named ‘dyonic salt’. This phase is analogue to the half-Skyrmion phase in the high-density Skyrme model and, for this reason, it has been argued to exhibit chiral symmetry restora-

tion. The instanton bag we discuss in the present paper can be considered as an extension of the dyonic salt phase to densities where the instantons start to populate the holographic direction. In a sense, this paper is a reconciliation of various approaches. Our state is also similar to the almost homogeneous state considered in [13], but with a different motivated ansatz.

The paper is organized as follows. In Section 2 we describe an instanton bag solution in flat space. In Section 3 we review some generic features of HQCD at finite density. In Section 4 we embed the instanton bag in HQCD and study the moduli stabilization. In Section 5 we review the top-down derivation of the Sakai-Sugimoto model. In Section 6 we discuss the phenomenon of chiral symmetry restoration at large densities. We conclude in Section 7.

2 An instanton bag from monopole walls

We consider a Yang-Mills (YM) theory in 5D Minkowski space-time with gauge group $SU(2)$. The action is

$$S_{YM5} = \int dt d^4x \frac{1}{4g^2} F_{\mu\nu}^a F^{\mu\nu a} . \quad (2.1)$$

Instantons correspond to particles with mass $8\pi^2/g^2$. We will consider solutions that are periodic in one direction, and thus we can formally compactify the x_3 direction on a circle of radius R_3 (we chose the direction 3 for later convenience). The sector of configurations that are also invariant along x_3 have the 4D Yang-Mills-Higgs (YMH) action

$$S_{YMH4} = \int dt dx_1 dx_2 dx_4 \frac{\pi R_3}{2g^2} (F_{\mu\nu}^a F^{\mu\nu a} + D\phi^a D\phi^a) , \quad (2.2)$$

where ϕ is just another name for A_3 . This is the first term in a Kaluza-Klein (KK) series expansion. The monopole wall studied in [14, 15] (see also [16–20]) is a solution of the Bogomoln'y equations $F_{ij} = \epsilon_{ijk} D_k \phi$ for the YMH action (2.1) and thus, lifted to 4D by keeping the fields x_3 independent, it is also a self-dual instanton solution satisfying $F = \tilde{F}$.

A sketch of the monopole wall solution is given in Figure 1. The wall is located at a fixed position in x_4 and is extended in the $x_{1,2,3}$ directions. The wall separates two phases, one on the left in which A_3 is constant and the field strength is vanishing, and the other on the right in which A_3 grows linearly with x_4 and the magnetic B field is constant. This is in the singular gauge in which the fields far from the wall are directed in a fixed direction in the $su(2)$ algebra, and Dirac string singularities are on the empty left side of the wall. The Bogomoln'y equation $B = F_{34}$ implies that A_3 is growing linearly as a function of x_4 . Details about the non-Abelian nature and its lattice structure are all contained in a small strip near the wall and can be neglected at large distances. When this solution is

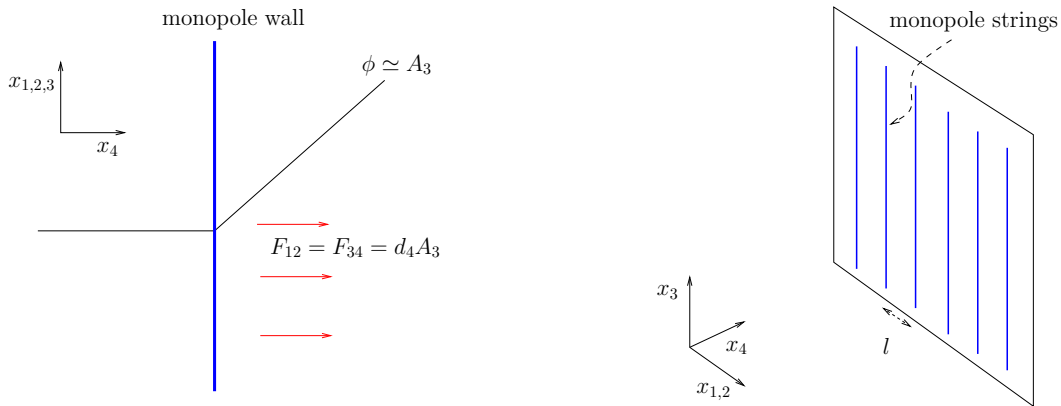


Figure 1: Monopole wall

lifted to 4D, the monopoles become monopole strings extended in the x_3 direction and the wall becomes a three-dimensional object.

The monopole wall solution is specified by the following set of parameters. The first is the area of the unit monopole lattice in the 1-2 plane. We name l the typical distance between the constituents monopoles and l^2 is the area of the unit lattice in the 1-2 plane. The magnetic field sourced by the wall is then related to the microscopic structure by

$$F_{12} = B t_{\text{su}(2)} \quad B = \frac{4\pi}{l^2}, \quad (2.3)$$

which is obtained by requiring that one unit of magnetic flux passes through each cell. Also, $t_{\text{su}(2)}$ is any normalized generator of $SU(2)$, for example $t_3 = \text{diag}(1/2, -1/2)$. In this singular gauge, the field F_{12} is constant far from the wall. The field A_3 is then given by

$$A_3|_{x_3 < 0} = 0 \quad \text{and} \quad A_3|_{x_3 > 0} = B x_3 t_{\text{su}(2)}. \quad (2.4)$$

The transverse thickness of the wall is of order

$$\delta \simeq \frac{1}{\sqrt{B}}, \quad (2.5)$$

being the scale where massive W bosons start to condense near the wall. As long as we are interested in length scales much greater than the lattice size l and the transverse thickness δ , the microscopic details of the monopole wall are not relevant. The monopole wall solution has a constant instanton charge and also constant energy density on the right side and zero on the left side.

A monopole wall in isolation is not enough to have finite instanton density in \mathbb{R}^3 . For this, we also need a wall of Kaluza-Klein monopoles, or a ‘KK monopole wall’. KK monopoles are solutions of YM equations on $\mathbb{R}^3 \times S^1$ with a non-trivial dependence on the compactified direction. They carry the same instanton charge of the monopole but an opposite magnetic charge. One instanton on $\mathbb{R}^3 \times S^1$

is then decomposable into one monopole plus one KK monopole [21–23], and the distance between the constituents is continuously connected with the scale modulus of the instanton. We will show that with a monopole wall and a KK monopole wall, we can create a configuration that has finite instanton density in a three-dimensional volume.

When the theory is compactified on a circle S^1 , so with the periodic identification $x_3 \equiv x_3 + 2\pi R_3$, we can make a gauge transformation that is topologically distinct from identity map

$$U(x_3) = e^{-ix_3 t_{\text{su}(2)}/R_3} . \quad (2.6)$$

This function goes from plus to minus the identity as x_3 completes its period. If the theory contains only adjoint fields, the gauge transformation (2.6) connecting the two elements of the centre of the group 1 and -1 is thus single valued. This gauge transformation shifts the gauge field by a constant

$$A_3 \longrightarrow A_3 - \frac{t_{\text{su}(2)}}{R_3} . \quad (2.7)$$

Therefore, the gauge field A_3 assumes value in a T-dual circle.

The KK monopole is an ordinary monopole transformed by a large-gauge transformation action plus a global gauge transformation that flips the sign of the generator $t_{\text{su}(2)} \rightarrow -t_{\text{su}(2)}$. The KK monopole has opposite sign relation between the instanton charge and the monopole charge. For example if we normalize so that the monopole has $(n_{\text{mon}}, n_{\text{inst}})$ charge equal to $(1/2, 1/2)$, the KK monopole has charges $(-1/2, 1/2)$. So the monopole together with a KK monopole has exactly the charge of an instanton $(0, 1)$. The asymptotic value of the Higgs field is $\phi \equiv A_3 \simeq t_{\text{su}(2)}/2R_3$, so the large-gauge transformation (2.7) plus the global transformation leave it invariant, and the monopole and KK monopole can be glued together. The global transformation flips the sign of both $d_r A_3$ and the magnetic field so that it does not affect the instanton charge.

The KK monopole wall can be obtained in a similar fashion by applying two transformations to the monopole wall. First we use the same large-gauge transformation (2.6) and then a π rotation in the x_3, x_4 plane: $x_{3,4} \rightarrow -x_{3,4}$ and $x_{1,2} \rightarrow x_{1,2}$. Gauge fields are vectors, so A_3 flips sign with this rotation. On the initial left side of the wall, the empty half $x_4 < 0$, the composition of the two transformations gives the following:

$$A_3 = 0 \longrightarrow -\frac{t_{\text{su}(2)}}{R_3} \longrightarrow +\frac{t_{\text{su}(2)}}{R_3} . \quad (2.8)$$

Moreover, the empty side is moved to the right side of the wall $x_4 > 0$. On the non-empty side, the one filled with magnetic field $x_4 > 0$, the field F_{12} remains unchanged because $x_{1,2}$ are not affected by the rotation. Also $d_4 A_3$ is unchanged because both d_4 and A_3 flip the sign. Therefore, both monopole wall and KK monopole wall satisfy the BPS equation with the same sign. The transformation

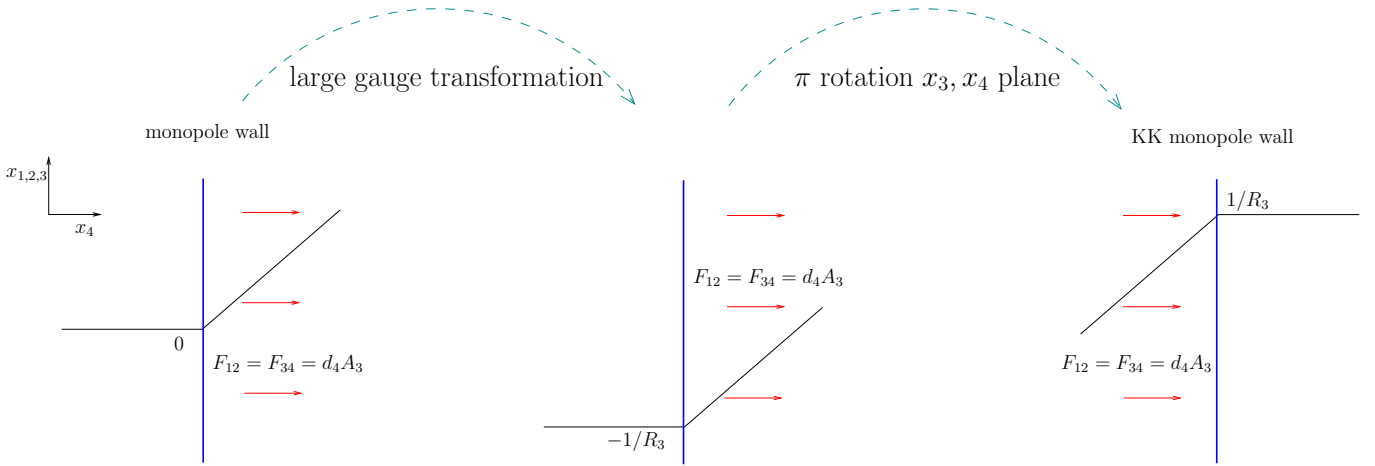


Figure 2: Sequence of transformations from monopole wall to KK monopole wall, first the large gauge transformation and then the π rotation in the x_3, x_4 plane.

we have described is exactly what we need to glue together the two walls. The two transformations are shown in Figure 2.

A monopole wall together with a KK monopole wall is capable of trapping the instanton charge in the middle of the two plates in the x_4 direction. They can be glued together since the B field and the derivative of A_3 have the same sign (see Figure 3). The microscopic scales are the lattice size l and the transverse

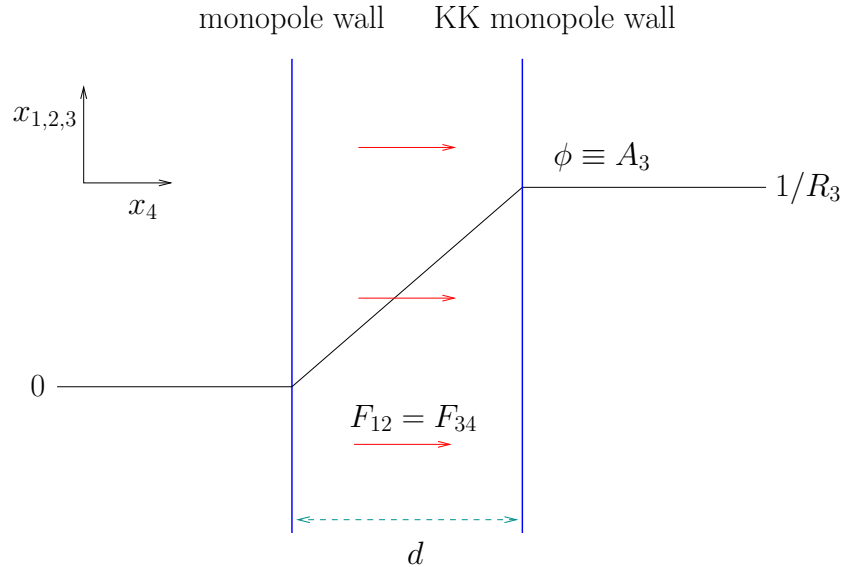


Figure 3: Monopole wall and KK monopole wall with instanton charge inside the two plates. The distance between the two walls is d . A_3 grows linearly between

the two walls from 0 to $1/R_3$. The BPS equation gives the following relation:

$$B = \frac{1}{dR_3} . \quad (2.9)$$

The instanton charge is still infinite in the directions $x_{1,2,3}$, but it is finite if interpreted as a density in the unit of three-dimensional volume. If we call Q the instanton density in a three-volume $dx_1dx_2dx_3$, we have the relation

$$Q = \int dx_4 \frac{1}{32\pi^2} F_{\mu\nu}^a \tilde{F}^{\mu\nu a} = \frac{B}{8\pi^2 R_3} . \quad (2.10)$$

We count the number of parameters of the solution. In total there are four parameters, l , B , R_3 , d , and two relations between them, (2.3), (2.9). Moreover, we want the instanton charge (2.10) to be fixed. We thus remain with a one-parameter family of solutions, which we can take to be the separation d . Rewriting everything as a function of the distance d , the coupling g , and the instanton charge density Q , we have the following set of relations:

$$\delta \simeq l = \frac{2\sqrt{\pi}}{\sqrt{B}} \quad R_3 = \frac{1}{2\pi\sqrt{2Qd}} \quad B = 2\pi\sqrt{\frac{2Q}{d}} . \quad (2.11)$$

The instanton bag we just discussed is very similar to the composite monopole walls studied in [17–20]. These solutions have an hyper-Kähler moduli space which, for two walls only, is 4 + 4-dimensional. The relative 4 moduli are distance d , a $U(1)$ relative phase, and a shift in the lattice positions of the two walls. The distance d is, for the present paper, the only modulus of these four that we will consider because the others affect only the microscopic structure.

For the bag approximation to be valid, we want to be in a regime in which we can neglect the microscopic structure of the wall, and thus we want the distance d to be much greater than l and δ . The most stringent condition of the two's is

$$d \gg l \quad \implies \quad \sqrt[4]{d^3 Q} \gg 1 . \quad (2.12)$$

Note that, even by keeping fixed Q and g , we can always reach a point in the moduli space where d is large enough to make the approximation valid. Yet another way to satisfy the condition is to increase Q while keeping d and g fixed.

It may be instructive to avoid the direct use of the Bogomoln'y equation (2.9) and use instead the minimization of the energy. The energy density per unit of volume $dx_1dx_2dx_3$ is

$$E = \frac{1}{2g^2} \int_{-d/2}^{d/2} dx_4 (F_{12}^a{}^2 + F_{34}^a{}^2) , \quad (2.13)$$

which then becomes

$$E = \frac{1}{2g^2} \left(dB^2 + \frac{64\pi^4 Q^2}{dB^2} \right) . \quad (2.14)$$

Minimizing by keeping Q fixed, we determine the value of dB^2 and the corresponding energy density

$$dB^2 = 8\pi^2 Q \quad E = \frac{8\pi^2 Q}{g^2} \quad , \quad (2.15)$$

where (2.9) is recovered, and one parameter between d and B disappears from E and remains thus a free modulus. This minimization strategy is the same we will use in Section 4 in the HQCD context, where the BPS equation is no longer valid.

A brane construction in string theory provides a very intuitive realization of the monopole wall [4, 24]. Monopoles are realized as D1-strings stretched between two D3-branes in type IIB string theory. We may take the D3 worldvolume to be stretched along the directions $x_{0,1,2,4}$ and the D1-string along $x_{0,3}$ with the two D3-branes separated in the x_3 direction. A monopole wall, in its simplest lattice realization, is an \mathbb{R}^2 periodic configuration, which we take along $x_{1,2}$. A series of transformation brings this configuration to a simpler system. First it can be turned into a D3-F1 system by an S-duality. Then, because we take a periodic configuration along x_{12} , we can compactify on a torus and perform T-duality on both directions. After these transformations, the D3-brane becomes a D1-string along the directions $x_{0,4}$, and the D1-string becomes a fundamental F1-string along $x_{0,3}$. The monopole wall is thus transformed into a web of connected D1 and F1 strings periodic in x_3 . The basic building block of this web is a string junction among a D1, an F1, and a third dyonic $(1, 1)$ -string with a certain angle in the $x_{3,4}$ plane dictated by the balance of the tensions. The instanton bag configuration is then described by the web in Figure 4. The junctions have to be placed in a periodic configuration in x_3 with the chain resulting from the KK monopole wall shifted of half-period respect to the chain coming from the monopole wall. To obtain the instanton bag we take this periodic web of string junctions, and perform all the previous dualities in reverse order. When we arrive at the original D3-D1 configuration, we perform another T-duality in the direction x_3 and we get the D4-D0 system.

As it is clear from the string web illustration in Figure 4, the monopole wall does not necessarily have to have a zero Higgs field on its empty side. The value of the Higgs field is in fact another parameter, which we call h (the existence of this extra freedom was observed in [17]). For $h \neq 0$, the monopole wall has an intrinsic tension given by

$$T = \frac{Bh}{g^2} = \frac{M_{mon}}{l^2} \quad , \quad (2.16)$$

which is consistent with the mass of a single BPS monopole with an asymptotic Higgs field equal to h

$$M_{mon} = \frac{4\pi h}{g^2} \quad . \quad (2.17)$$

The two configurations in Figure 4 have exactly the same energy. What is gained from the monopoles mass is lost from the fact that the two walls are closer.

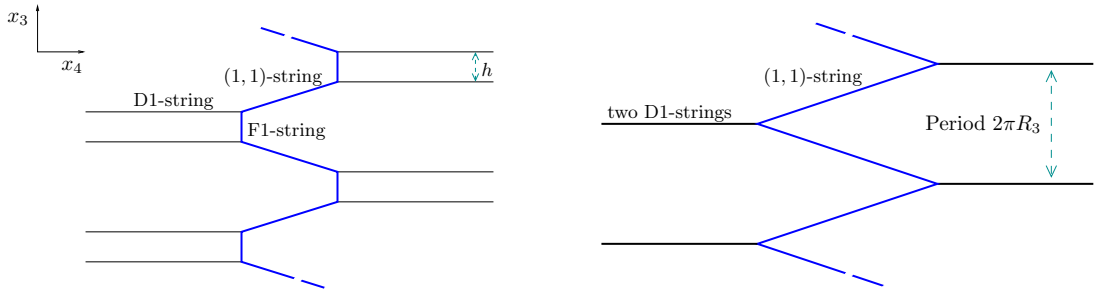


Figure 4: Web of string junctions in the $x_{3,4}$ plane. The basic constituent is the three string junction D1-F1-(1,1). The structure is periodic in the x_3 direction. The second is the web for the limit of coincident D1-strings. This configuration corresponds to the instanton bag of Figure 3.

In HQCD, this is no longer a free modulus, but must enter the minimization procedure like d and B . We will see that the $h = 0$ is, in general, the energetically favourite state.

We conclude this section with a discussion of the gauge in which we want to prepare our system. When we embed the monopole wall and KK monopole wall pair in holography, we want to choose a gauge that is the most convenient for the AdS/CFT dictionary. Usually, this is the gauge in which the gauge field is zero at the UV boundary, which are the two asymptotic limits $x_4 \rightarrow \pm\infty$.¹ The gauge we used for the previous discussion is not of this kind because there are Dirac strings singularities, one for every period of the monopole wall and KK monopole wall. To eliminate the Dirac strings we can go to the analogue of the hedgehog gauge for the 't Hooft-Polyakov monopole. In the middle of the two walls the gauge transformation is a function $U(x_1, x_2)$ so that the adjoint field $U(x_1, x_2)t_{\text{su}(2)}U(x_1, x_2)^{-1}$ winds around $SU(2)/U(1)$ once for every period of the wall lattice. This is particularly relevant for later application in HQCD. The magnetic fields F_{12} and F_{34} fluctuate around the $\text{su}(2)$ algebra so that every wave coming from the empty side of the wall in a fixed $\text{su}(2)$ generator (which in HQCD are dual to the vector meson states in a given isospin state) interacts with some magnetic field. This gauge is convenient to check that the instanton charge is equal to the flux of the Chern-Simons current

$$K^\mu = \frac{1}{16\pi^2} \epsilon^{\mu\nu\rho\sigma} \left(A_\nu^a F_{\rho,\sigma}^a + \frac{2}{3} \epsilon_{abc} A_\nu^a A_\rho^b A_\sigma^c \right), \quad (2.18)$$

We take a 4D volume as in Figure 5 that encloses part of the instanton bag. The gauge field vanishes at the left side of the monopole wall and at the right side of the KK monopole wall. So the Chern-Simons flux can escape only through the volumes 1-3-4, 2-3-4, and 1-2-4 inside the two walls. No term from ϵ_{abc} in the

¹If the gauge field is not zero at the boundary but gauge equivalent to zero, and if we do not want to interpret it as a source, the AdS/CFT dictionary also must be modified accordingly.

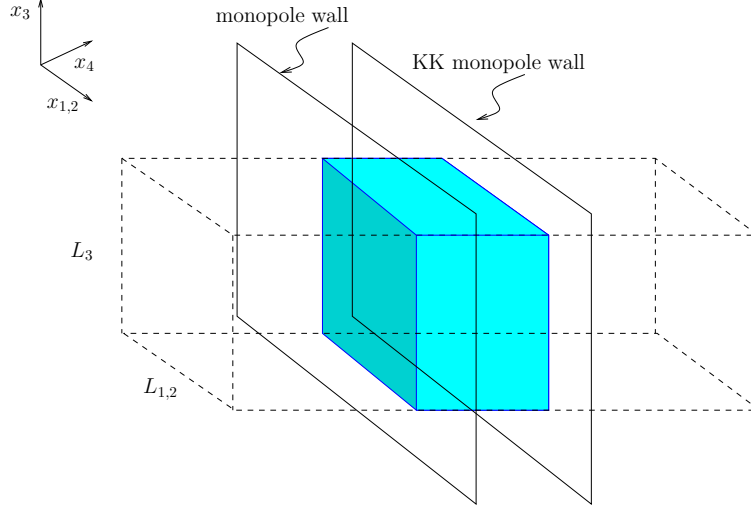


Figure 5: Check of the Chern-Simons flux.

Chern-Simons current gives any contribution. Moreover there is no contribution from the 1-2-4 volume. We just have to compute the flux from 1-3-4 and 2-3-4. The total instanton charge I is then

$$I = \int dx_i dx_3 dx_4 \frac{1}{8\pi^2} A_i^a F_{34}^a = \frac{B}{8\pi^2 R_3} L_1 L_2 L_3, \quad (2.19)$$

where $i = 1, 2$. This is consistent with the instanton density (2.10).

3 HQCD and finite baryon density

The Sakai-Sugimoto model, at low energy, consists of a $U(2)$ gauge theory in the following 5D warped metric background:

$$ds^2 = H(z) dx_\mu dx^\mu + H(z)^{-1} dz^2 \quad H(z) = \left(1 + \frac{z^2}{z_0^2}\right)^{2/3}. \quad (3.1)$$

The length scale z_0 is related to the inverse of the dynamical scale in the dual QCD-like theory. From now on we set $z_0 = 1$. The action is a sum of the Yang-Mills term plus a $U(2)$ Chern-Simons term:

$$S = -\frac{N_c \lambda}{216\pi^3} \int d^4 x dz \sqrt{-g} \frac{1}{2} \text{tr} (\mathcal{F}_{\Gamma\Delta} \mathcal{F}^{\Gamma\Delta}) + \frac{N_c}{24\pi^2} \int d^4 x dz \omega_5(\mathcal{A}). \quad (3.2)$$

We use the indices conventions as follows: $\Gamma, \Delta, \dots = 0, 1, 2, 3, z$; $\mu, \nu, \dots = 0, 1, 2, 3$; $I, J = 1, 2, 3, 4$ and $i, j, \dots = 1, 2, 3$. The factors N_c and λ are respectively the number of colours and the 't Hooft coupling of the dual theory. We can decompose the gauge field into non-Abelian and Abelian components $U(2) = SU(2) \times U(1)$:

$$\mathcal{A}_\Gamma = A_\Gamma + \frac{1}{2} \hat{A}_\Gamma \quad \mathcal{F}_{\Gamma\Delta} = F_{\Gamma\Delta} + \frac{1}{2} \hat{F}_{\Gamma\Delta}. \quad (3.3)$$

In the following, we are only interested only in static configurations, so we restrict to the following ansatz:

$$A_I, \hat{A}_0 = A_I(x_I), \hat{A}_0(x_I) \quad A_0, \hat{A}_I = 0, 0 . \quad (3.4)$$

The action is then reduced to

$$\begin{aligned} \mathcal{S} = & \int d^4x dz \left\{ \frac{1}{2H^{1/2}} (\partial_i \hat{A}_0)^2 + \frac{H^{3/2}}{2} (\partial_z \hat{A}_0)^2 - \frac{1}{2H^{1/2}} \text{tr} (F_{ij}^2) - H^{3/2} \text{tr} (F_{iz}^2) \right\} \\ & + \frac{1}{\Lambda} \int d^4x dz \hat{A}_0 \text{tr} (F_{IJ} F_{KS}) \epsilon^{IJKS} , \end{aligned} \quad (3.5)$$

where we have rescaled for convenience the action and the 't Hooft coupling as

$$\mathcal{S} = \frac{64\pi^2}{\Lambda N_c} S \quad \text{and} \quad \Lambda = \frac{8\lambda}{27\pi} . \quad (3.6)$$

For large 't Hooft coupling, the Chern-Simons term is parametrically suppressed with respect to the Yang-Mills term. The instanton in the large Λ limit can thus be approximated by a BPS ansatz [25, 26]

$$A_I = -\sigma_{IJ} x_J \frac{1}{\rho^2 + l^2} \quad (3.7)$$

with $\sigma_{ij} = \epsilon_{ijk} \sigma_k$ and $\sigma_{iz} = -\sigma_{zi} = \sigma_i$. The size of the instanton l is then obtained by minimizing the energy restricted to the BPS moduli space. This gives

$$l = \frac{3^{1/4} 2}{5^{1/4} \Lambda^{1/2}} \quad \text{and} \quad \mathcal{E} = 8\pi^2 \left(1 + \frac{8}{15^{1/2} \Lambda} + \dots \right) . \quad (3.8)$$

At large Λ , the size of the instanton is much smaller than the curvature scale of the metric, which is why the BPS profile function provides a good approximation of the true solution, at least in the almost-flat region of the metric. Moreover, the correction to the BPS mass is a sub-leading term of order $\mathcal{O}(1/\Lambda)$. The solution flows exactly to the BPS for $\Lambda \rightarrow \infty$ but only in rescaled coordinates [27], so the large-distance properties are not captured by the BPS ansatz. Large distance properties are not relevant for high-density QCD due to the small distance between baryons will not discuss them in this paper.

At finite densities, the instantons are distributed on a lattice configuration, and they begin to populate the 3D space by all sitting at the bottom of the gravitational potential at $z = 0$. Their average distance is thus $d = Q^{-1/3}$, where Q is the 3D instanton density. This configuration remains valid as long as the typical distance d is larger than the size of the single instantons, and thus for densities $Q \ll \Lambda^{3/2}$. In this regime, the energy density is dominated by the BPS term, and thus linear in Q . In the ensemble in which we keep the chemical potential fixed, a phase transition to hadronic matter is expected to take place when the average distance is of order of the curvature scale, thus $Q \simeq 1$. This is when the attractive

force due to the pion-pion tail is comparable with the Coulomb repulsive force [28]. Above this scale $Q \gg 1$, the attractive force becomes irrelevant with respect to the Coulomb repulsive force. The Coulomb interaction correction, for any couple of them at distance \tilde{d} , is order $E_{\text{Coulomb}} \propto 1/\Lambda\tilde{d}^2$ and this is valid for $l \ll \tilde{d} \ll 1$. We can compute the energy density of the 3D lattice as a sum of the mass of the single constituents plus the correction due to the Coulomb interaction:

$$\mathcal{E} = 8\pi^2 Q \left(1 + \mathcal{O} \left(\frac{Q}{\Lambda^2} \right) \right) . \quad (3.9)$$

Note that, for the Coulomb term, we summed the $1/\tilde{d}^2$ term for every pair of constituents, taking as cutoff $\tilde{d} \simeq 1$, where the Coulomb law is certainly modified by the metric curvature. The Coulomb correction becomes comparable with the BPS energy at densities of order $Q \simeq \Lambda^2$, which are much bigger than $\Lambda^{3/2}$.

When the instanton density becomes of order $Q \simeq \Lambda^{3/2}$, two interesting things happen almost simultaneously. First, the instanton lattice is no longer diluted because the typical inner distance becomes comparable with the instanton size $d \simeq l$. Second, the instantons begin to climb the holographic direction as we are going to see with the following simple estimate. We can estimate the force acting on each single instantons. The first force is the gravitational one, $F_{\text{Grav}} \propto -\Lambda z$, where z is the linear displacement around the bottom of the gravitational potential. Then there is a Coulomb force due to the surrounding instantons in the 3D lattice. This force, projected in the z component, is proportional to z/\tilde{d}^4 for any pair of instantons. The total force is thus $F_{\text{Coulomb}} \propto +Q^{4/3}z$. This force is pulling the instantons away from the bottom of the gravitational potential because it is repulsive. The instantons begin to move away from the bottom of the gravitational potential when the two forces are comparable $F_{\text{Grav}} \simeq F_{\text{Coulomb}}$. This condition is the same as the breaking of the diluted approximation. The fact that these two changes both happen at the densities $Q \simeq \Lambda^{3/2}$ is not a coincidence; it has also been discussed in [29] and observed in the toy model [1]. The agents that stabilize the instanton radius are, in fact, the same that decide when the instanton lattice prefers to move the holographic direction.

At densities $Q \simeq \Lambda^{3/2}$, the instantons start to fill the holographic direction as well. After that, another transition happens at higher densities $Q \simeq \Lambda^2$. Assuming the average distance remains of the order of the instanton scale $d \simeq l$, the instanton 4D lattice boundary reaches the curvature scale $z \simeq 1$, which is when Q is of order Λ^2 . This is also the density when the Coulomb energy becomes comparable with the BPS energy (3.9), and thus the energy density strongly deviates from the BPS bound. These phases are summarized in Figure 6.

The information we extracted so far is based on qualitative estimates. To find the actual instanton solution for the high-density phase is a much harder task. A 4D instanton lattice is specified by many parameters: the 3D lattice strata, the relative orientation of the instantons in the internal space, the sizes of the instantons, and the depth of the various layers in the holographic direction z . For densities $Q \ll \Lambda^2$, the problem simplifies since we can use a BPS ansatz

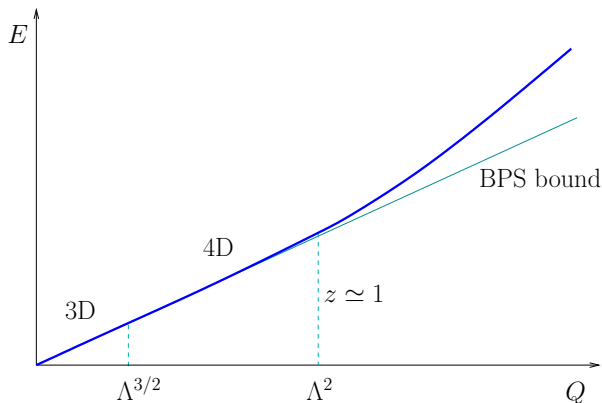


Figure 6: Generic expectation for the energy density of the HQCD phases as function of instanton density Q .

and minimize the energy restricted to the BPS moduli space. But even in this simplified case, the problem remains difficult to solve in full generality. Some results of the self-dual configurations periodic on \mathbb{T}^3 and \mathbb{T}^4 have been obtained using a version of the ADHM transform [30]. But the energy minimization would require knowledge of the actual gauge fields and not just the ADHM data.

Our strategy in the rest of the paper is to use the instanton bag discussed in Section 2 as an ansatz for the high-density phase. For the instanton bag approximation, we can compute the fields and thus perform the energy minimization. At the moment, we do not have sufficient control over other possible instanton configurations to compute their energy and thus decide which is the actual minimum for the high-density phase.

4 Instanton bag embedded in the Sakai-Sugimoto model

We now embed the instanton bag studied in Section 2 into the Sakai-Sugimoto model.

We first use the BPS ansatz and find the best values of the moduli that minimize the energy density at a fixed instanton density. The BPS solution in flat space has two free moduli, the wall separation d and Higgs field h . We now parametrize them with $\pm z_w$, which are the positions of the monopole wall and KK-monopole wall in the z direction, and Δ , which is the amount of instanton charge carried by the walls as a delta function. The relation

$$Q = \frac{B^2 z_w}{4\pi^2} + \Delta \quad (4.1)$$

is valid for a self-dual solution and gives the instanton charge Q as function of z_w , B and Δ . We use it later to express B as function of the other parameters.

The action (3.5) inside the two walls is reduced to

$$\frac{\mathcal{S}}{V_3} = \int dt \int_{-z_w}^{z_w} dz \left\{ \frac{H^{3/2}}{2} (\partial_z \hat{A}_0)^2 - \frac{B^2(1+H^2)}{2H^{1/2}} + \frac{2}{\Lambda} \hat{A}_0 B^2 \right\}. \quad (4.2)$$

From this, we find the equation for the Abelian electric potential \hat{A}_0 :

$$\partial_z (H^{3/2} \partial_z \hat{A}_0) - \frac{2}{\Lambda} B^2 = 0. \quad (4.3)$$

The solution for the electric field inside the walls is thus

$$\partial_z \hat{A}_0 = \frac{2B^2 z}{\Lambda(1+z^2)} \quad \text{for} \quad |z| \leq z_w. \quad (4.4)$$

The solution outside the walls is given by the solution of the equation without sources, matched with (4.4) at $z = z_w$:

$$\partial_z \hat{A}_0 = \frac{8\pi^2 Q}{\Lambda(1+z^2)} \quad \text{for} \quad |z| > z_w. \quad (4.5)$$

The energy density is given by the sum of three contributions

$$\mathcal{E} = \int_0^{z_w} \left(H^{3/2} (\partial_z \hat{A}_0)^2 + \frac{B^2(1+H^2)}{H^{1/2}} \right) + 8\pi^2 \Delta (1+z_w^2) + \int_{z_w}^{\infty} H^{3/2} (\partial_z \hat{A}_0)^2 \quad (4.6)$$

with $A_0(z)$ given by (4.4) and (4.5). We evaluate the integrals, and then expand in series of z_w , since the self-dual approximation is supposed to be valid only for $z_w \ll 1$. The result is

$$\begin{aligned} \mathcal{E}(Q; z_w, \Delta) &= 8\pi^2 Q - \frac{64(2\pi^4 Q^2 + 2\pi^4 Q \Delta - \pi^4 \Delta^2)}{3\Lambda^2} z_w + \\ &+ \frac{8\pi^2(Q + 8\Delta)}{9} z_w^2 + \dots \end{aligned} \quad (4.7)$$

This energy density has to be minimized with respect to z_w and Δ by keeping the instanton charge Q fixed. The solution is given by

$$z_w = \frac{24\pi^2 Q}{\Lambda^2} \quad \Delta = 0. \quad (4.8)$$

The energy density evaluated at the minimum is then

$$\mathcal{E}(Q) = 8\pi^2 Q \left(1 + \frac{4\pi^3 Q}{\Lambda^2} - \frac{64\pi^4 Q^2}{\Lambda^4} + \dots \right). \quad (4.9)$$

Note that the dominant term is the BPS bound, and the corrections are small if $Q \ll \Lambda^2$. This is also the regime in which $z_w \ll 1$. Moreover, the bag approximation is valid when the wall microscopic structure is much smaller than z_w (see

(2.12)) and thus, using (4.8), becomes equivalent to $Q \gg \Lambda^{3/2}$. Therefore, the BPS and bag approximations are both valid in the region of instanton densities $\Lambda^{3/2} \ll Q \ll \Lambda^2$.

When z_w becomes of order one, we can no longer use the self-dual approximation, although we can still use the instanton bag approximation. For this, we have to solve the profile function for $A_3(z)$ as it is generally modified by the metric curvature and is no longer linear in z . The relation (4.1) is now given in more generality by the following:

$$Q = \frac{B}{8\pi^2} \int_{-z_w}^{z_w} \partial_z A_3 + \Delta . \quad (4.10)$$

The action density between the two walls is

$$\frac{\mathcal{S}}{V_3} = \int dt \int_{-z_w}^{z_w} dz \left\{ \frac{H^{3/2}}{2} (\partial_z \hat{A}_0)^2 - \frac{B^2}{2H^{1/2}} - \frac{H^{3/2}}{2} (\partial_z A_3)^2 + \frac{2}{\Lambda} \hat{A}_0 B \partial_z A_3 \right\} , \quad (4.11)$$

from which we derive the equations for \hat{A}_0 and A_3 :

$$\partial_z \left(H^{3/2} \partial_z \hat{A}_0 \right) - \frac{2}{\Lambda} B \partial_z A_3 = 0 \quad (4.12)$$

$$\partial_z \left(H^{3/2} \partial_z A_3 - \frac{2}{\Lambda} \hat{A}_0 B \right) = 0 . \quad (4.13)$$

The second one can be integrated

$$\partial_z A_3 = \frac{2\hat{A}_0 B - C\Lambda}{\Lambda H^{3/2}} , \quad (4.14)$$

where C is an arbitrary integration constant. The equation (4.12), together with the boundary conditions $\hat{A}_0(0) = \partial_z \hat{A}_0(0) = 0$, gives the solutions for \hat{A}_0

$$\hat{A}_0 = \frac{C\Lambda}{2B} \left(1 - \cosh \left(\frac{2B \tan^{-1}(z)}{\Lambda} \right) \right) . \quad (4.15)$$

The solution for $\partial_z A_3$ is

$$\partial_z A_3 = \frac{C}{H^{3/2}} \cosh \left(\frac{2B \tan^{-1}(z)}{\Lambda} \right) . \quad (4.16)$$

The relation (4.10) can now be written as

$$Q = \frac{C\Lambda}{8\pi^2} \sinh \left(\frac{2B \tan^{-1}(z_w)}{\Lambda} \right) + \Delta \quad (4.17)$$

Outside the walls, A_3 is constant while \hat{A}_0 is given by

$$\hat{A}_0 = c_1 - C \sinh \left(\frac{2B \tan^{-1}(z_w)}{\Lambda} \right) \tan^{-1}(z) , \quad (4.18)$$

where c_1 is a constant that we will not need in the next.

The energy density is then given by

$$\begin{aligned} \mathcal{E} = & \int_0^{z_w} \left(H^{3/2} (\partial_z \hat{A}_0)^2 + \frac{B^2}{H^{1/2}} + H^{3/2} (\partial_z A_3)^2 \right) \\ & + \frac{\Delta(1+z_w^2)}{\pi^2} + \int_{z_w}^{\infty} H^{3/2} (\partial_z \hat{A}_0)^2 . \end{aligned} \quad (4.19)$$

We can use the relation (4.17) to write the integration constant C as function of the other parameters, and then the energy density becomes

$$\begin{aligned} \mathcal{E}(Q; B, z_w, \Delta) = & \frac{16\pi^4(Q-\Delta)^2 \sinh\left(\frac{4B \tan^{-1}(z_w)}{\Lambda}\right)}{B\Lambda \left(\sinh\left(\frac{2B \tan^{-1}(z_w)}{\Lambda}\right)\right)^2} + B^2 \int_0^{z_w} \frac{1}{(1+z^2)^{1/3}} + \\ & + \frac{\Delta(1+z_w^2)}{\pi^2} + \frac{64\pi^4(Q-\Delta)^2}{\Lambda^2} \left(\frac{\pi}{2} - \tan^{-1}(z_w)\right) \end{aligned} \quad (4.20)$$

This is the function that has to be minimized with respect to the three parameters B, z_w, Δ , while keeping Q fixed. With the following convenient rescaling

$$B = b\Lambda \quad Q = q\Lambda^2 , \quad (4.21)$$

we can write the functional (4.20) as

$$\begin{aligned} \frac{1}{\Lambda^2} \mathcal{E}(q; b, z_w) = & \frac{16\pi^4 q^2 \sinh(4b \tan^{-1}(z_w))}{b (\sinh(2b \tan^{-1}(z_w)))^2} + b^2 \int_0^{z_w} \frac{1}{(1+z^2)^{1/3}} + \\ & + 64\pi^4 q^2 \left(\frac{\pi}{2} - \tan^{-1}(z_w)\right) . \end{aligned} \quad (4.22)$$

Numerical examples, for a given value of q , shows that the minimum always exists and is at $\Delta = 0$ and for some finite value of B, z_w .

An analytic solution to the minimization of (4.22) can be obtained in the limit $z_w \gg 1$. For this, we can first minimize (4.22) with respect to z_w by keeping only the dominant terms in a large z_w expansion

$$z_w = \left(\frac{8q \coth(b\pi)}{b}\right)^{3/2} \quad \text{for} \quad z_w \gg 1 . \quad (4.23)$$

We then have to minimize

$$\frac{1}{\Lambda^2} \mathcal{E}(q; b) = \frac{32\pi^4 q^2 \coth(b\pi)}{b} + 8\sqrt{2} b^{3/2} \pi (q^2 (\coth(b\pi))^2)^{1/4} + \frac{b^2 \sqrt{\pi} \Gamma\left[-\frac{1}{6}\right]}{2\Gamma\left[\frac{1}{3}\right]} \quad (4.24)$$

with respect to b . By considering only the dominant terms in the large q limit, we obtain the result

$$b = 2 \left(\frac{\pi^2 q}{32/3}\right)^{3/5} \quad \text{and} \quad z_w = 8 \left(\frac{3q}{\pi^3}\right)^{3/5} \quad \text{for} \quad q \gg 1 , \quad (4.25)$$

and the energy density is

$$\mathcal{E}(Q) = 80 \left(\frac{\pi^{14} Q^7}{3^3 \Lambda^4} \right)^{1/5} \quad \text{for} \quad Q \gg \Lambda^2 . \quad (4.26)$$

Note that the derivative with respect to Δ is positive:

$$\left. \frac{\partial \mathcal{E}}{\partial \Delta} \right|_{\Delta=0} \simeq + \frac{z_w^2}{\pi^2} - \frac{64 \pi^5 Q}{\Lambda^2} > 0 \quad \text{for} \quad Q \gg \Lambda^2 . \quad (4.27)$$

This limit $Q \gg \Lambda^2$ is exactly the opposite of the BPS limit previously considered.

The minimization can be performed numerically for any value of Q . The results are shown in Figures 7 and 8 and are confronted both with the small Q and large Q approximations.

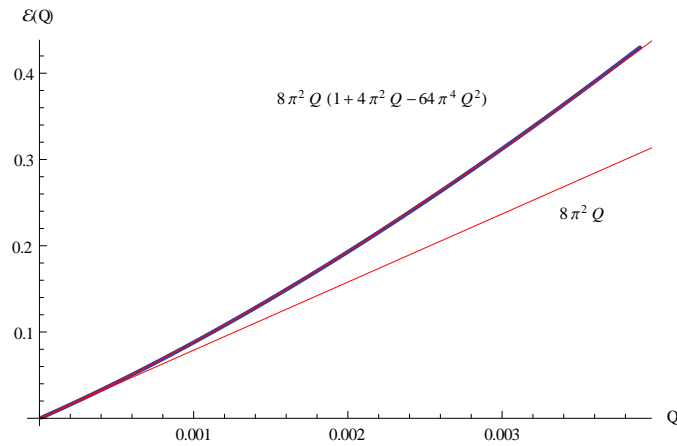


Figure 7: Numerical plot of $\mathcal{E}(Q)$ for small values of Q obtained from the minimization of (4.22). This confirms the expectation from the BPS approximation (4.9).

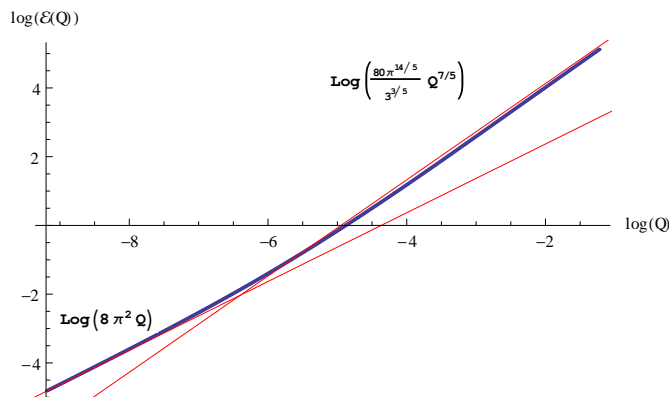


Figure 8: Numerical solution of $\mathcal{E}(Q)$ in a log-log plot. This shows the interpolation between the almost BPS limit for small Q and the asymptotic solution (4.26) for large Q .

We can consider a local inertial frame by zooming in closer to the monopole wall. In the new coordinates

$$\tilde{x}_\mu = H(z_w)^{1/2} x_\mu \quad \tilde{z} = \frac{z - z_w}{H(z_w)^{1/2}}, \quad (4.28)$$

the metric is locally Minkowski

$$ds^2 \simeq d\tilde{x}_\mu d\tilde{x}^\mu + d\tilde{z}^2, \quad (4.29)$$

and this is valid as long as $|\tilde{z}|$ is much smaller than the metric curvature radius, which, for $z_w \gg 1$, is the condition

$$|\tilde{z}| \ll \frac{1}{|R|^{1/2}} \simeq \frac{3z_w^{1/3}}{2\sqrt{13}}. \quad (4.30)$$

In this frame, the fields close to the wall are

$$\begin{aligned} F_{\tilde{z}\tilde{3}} &= F_{z3} = \frac{8\pi^2 Q}{\Lambda z_w^2} = \frac{\pi^{28/5} \Lambda^{7/5}}{3^{6/5} 8Q^{1/5}} \\ F_{\tilde{1}\tilde{2}} &= \frac{B}{H(z_w)} = \frac{\pi^{18/5} \Lambda^{7/5}}{3^{6/5} 8Q^{1/5}}. \end{aligned} \quad (4.31)$$

The monopole wall lattice period \tilde{l} and the transverse thickness $\tilde{\delta}$ are given by

$$\tilde{l} = \frac{1}{\sqrt{F_{\tilde{1}\tilde{2}}}} \quad \tilde{\delta} = \frac{1}{\sqrt{F_{\tilde{z}\tilde{3}}}} \quad (4.32)$$

and are always smaller than the curvature radius. This justifies the approximation made before of neglecting the microscopic structure of the walls.

5 Embedding in string theory

Now we move to full string version of Sakai-Sugimoto [31]. First we briefly review the brane construction and the near-horizon geometry. The SS model starts with the intersection of D4, D8 and anti-D8 branes in type IIA string theory. The gauge theory with group $SU(N_c)$ is defined on the D4-branes, which are extended along the directions $x_{0,1,2,3,5}$, and the N_f flavours are provided by the D8-branes and anti-D8-branes extended along the directions $x_{0,1,2,3,5,6,7,8,9}$. This brane intersection leaves only massless chiral fermion with one gauge and one flavor index in the low-energy theory. Moreover the direction x_5 is compactified with anti-periodic boundary conditions for fermions on a circle with radius R_5 [32]. With this compactification, the low-energy of the D4 is exactly that of QCD in $3 + 1$ dimension with N_f massless fermions.

The next step is to take large N_c and large λ limits and go to near-horizon geometry of the D4-branes. The D4-branes disappear and leave a curved AdS_5

geometry compactified on x_5 plus an S^4 sphere with N_c units of RR flux. The D8-branes remain as physical branes in this background. The geometry, the field strength and the dilaton are given by

$$\begin{aligned} ds^2 &= \left(\frac{u}{L}\right)^{3/2} (dx_\mu dx^\mu + h(u) dx_5^2) + \left(\frac{L}{u}\right)^{3/2} \left(\frac{du^2}{h(u)} + u^2 d\Omega_4^2\right) \\ F_4 &= \frac{(2\pi)^3 \alpha'^{3/2} N_c}{V_4} \text{vol}(S^4) & e^\phi &= g_s \left(\frac{u}{L}\right)^{3/4} \end{aligned} \quad (5.1)$$

with

$$h(u) = 1 - \left(\frac{u_0}{u}\right)^3 \quad (5.2)$$

This is a cigar-like topology in the two-dimensional subspace x_5, u (see Figure 9). It is like a Euclidean Schwarzschild black hole, with x_5 playing the role of the Euclidean time. The holographic direction is u , and both $u \rightarrow \infty$ correspond to the UV limit of the boundary theory. The cigar topology implies that the two stacks of D8 and anti-D8 branes are continuously joined together at the tip of the cigar; this is the geometric realization of chiral symmetry breaking.

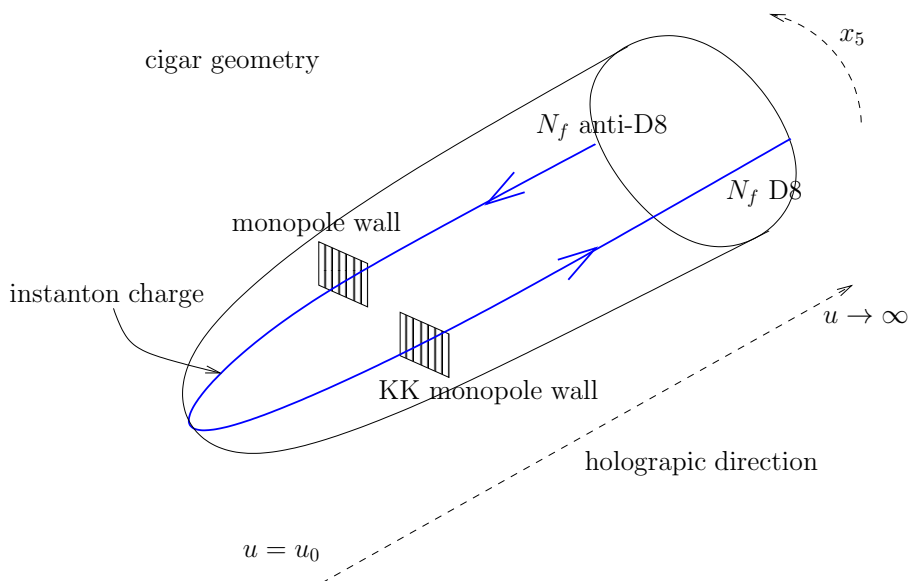


Figure 9: Geometric realization of confinement and chiral symmetry breaking in the Sakai-Sugimoto model and the embedded instanton bag on the $D8$'s worldvolume.

We now recall the relation between bulk and boundary theories. The dual gauge theory is defined by the gauge couplings g_{YM4} and g_{YM5} , the number of colors N_c , the compactification radius R_5 , and the 't Hooft coupling λ related by the following:

$$g_{YM4}^2 = \frac{g_{YM5}^2}{2\pi R_5} \quad \lambda = g_{YM4}^2 N_c . \quad (5.3)$$

The dynamical scale is given by

$$\Lambda_{QCD} = \frac{1}{R_5} e^{-cost/\lambda} \quad (5.4)$$

which means that the low-energy QCD is hierarchically separated from the Kaluza-Klein modes only for $\lambda \ll 1$. This is one limitation of the $\lambda \rightarrow \infty$ limit in the SS model. Thus the bulk string theory has parameters g_s, α', L, u_0 , and R_5 , which is shared. The absence of any conical singularity at the cigar tip gives the relation

$$\frac{1}{R_5^2} = \frac{9u_0}{4L^3} . \quad (5.5)$$

We then have three parameters to be matched between bulk and boundary. The dictionary is given by the following three relations

$$\frac{L^3}{\alpha'} = \frac{\lambda R_5}{2} \quad \frac{u_0}{\alpha'} = \frac{2\lambda}{9R_5} \quad g_s \sqrt{\alpha'} = \frac{\lambda R_5}{2\pi N_c} . \quad (5.6)$$

Note that only three out of the four parameters, L, u_0, g_s, α' , are need to define the boundary parameters N_c, λ, R_5 .

To maintain string theory at weak coupling, we need the curvature of the bulk to be small with respect to the string scale and thus the 't Hooft coupling to be large

$$\frac{\sqrt[4]{L^3 u_0}}{\sqrt{\alpha'}} \gg 1 \quad \implies \quad \sqrt{\lambda} \gg 1 \quad (5.7)$$

Moreover the string coupling has to be small

$$g_s \left(\frac{u_0}{L} \right)^{3/4} \gg 1 \quad \implies \quad \sqrt{\lambda^{3/2}/N_c} \ll 1 . \quad (5.8)$$

There is always a scale u_{UV} above which string theory is no longer weakly coupled. For this, we need a further restriction on N_c and λ :

$$\frac{u_{UV}}{u_0} \simeq \frac{N_c^{4/3}}{\lambda^2} \gg 1 . \quad (5.9)$$

The low-energy theory on the D8-branes is the non-Abelian DBI action plus a WZ term. Since the D8 and anti-D8 are continuously connected, we can write an action on a single extended stack of N_f D8-branes. We will mostly focus on the $N_f = 2$ case. The DBI action, in the weak field limit is just the Yang-Mills action, so that:

$$\begin{aligned} S = & -k \int d^4 x du \frac{u^{5/2}}{h(u)^{1/2}} \frac{1}{2} \text{tr} \left(\left(\frac{L}{u} \right)^3 \mathcal{F}_{\mu\nu} \mathcal{F}^{\mu\nu} + 2h(u) \mathcal{F}_{\mu\nu} \mathcal{F}^{\mu\nu} \right) + \mathcal{O}(\mathcal{F}^4) \\ & + \frac{N_c}{24\pi^2} \int \omega_5^{N_f}(\mathcal{A}) , \end{aligned} \quad (5.10)$$

where we raised indices with $\eta^{\Gamma\Delta}$, and the coefficient k is given by

$$k = \frac{L^{3/2}}{2^4 3 \pi^4 g_s \alpha'^{5/2}} . \quad (5.11)$$

This can be written as a theory living on an effective 5D effective metric which takes into account the effect of the dilaton:

$$ds = \frac{u^2}{u_0^2} dx^2 + \frac{L^3}{u_0^2 u h(u)} du^2 . \quad (5.12)$$

We can change variables from u to z with

$$1 + \frac{z^2}{z_0^2} = \frac{u^3}{u_0^3} \quad \text{with} \quad z_0^2 = \frac{4L^3}{9u_0} = R_5^2 . \quad (5.13)$$

This brings the metric to the form (3.1), and the action (5.10) to (3.2) in the x^μ, z coordinates in units $z_0 = R_5 = 1$.

Figure 9 how the instanton bag solution is embedded in the D8's world-volume. The terms (5.10) are a truncation of the DBI action to the first YM term. The original DBI action for the D8 brane is

$$S_{DBI} = T_8 \int d^9 x e^{-\phi} \text{tr} \sqrt{-\det(g_{\Gamma\Delta} + 2\pi\alpha' \mathcal{F}_{\Gamma\Delta})} . \quad (5.14)$$

To check if the truncation of the DBI action to the YM term is a good approximation, we have to check if the three corrections

$$\frac{(\alpha' B)^2}{g_{11} g_{22}} , \quad \frac{(\alpha' F_{3u})^2}{g_{33} g_{uu}} , \quad \frac{(\alpha' \hat{F}_{u0})^2}{g_{00} g_{uu}} \quad (5.15)$$

are negligible for any u . In the almost-BPS limit, that is $Q \ll \Lambda^2$, the first two in (5.15) are both of order one. So, as it happens for an instanton in isolation, the YM term receives order one corrections from the higher derivative terms. This is mitigated by the fact that the self-dual solutions are also solutions of the DBI action in flat space [33]. Even in the large $Q \ll \Lambda^2$ limit, computed on the solution (4.25), these higher derivative corrections remain non-negligible.

In the effective metric (3.1) the full DBI plus CS action is

$$\mathcal{S} = - \int d^4 x dz C \text{tr} \sqrt{-\det \left(g_{\Gamma\Delta} + \frac{2}{C^{1/2}} \mathcal{F}_{\Gamma\Delta} \right)} + \frac{8}{3\Lambda} \int d^4 x dz \omega_5(\mathcal{A}) \quad (5.16)$$

where

$$C = \frac{\Lambda^2}{16(1+z^2)^{1/2}} , \quad (5.17)$$

and we used the same rescaling as (3.6). For the almost-BPS regime, from (4.1) and (4.8), the non-Abelian field is $B = \Lambda/\sqrt{6}$ inside the instanton bag. The correction from the higher derivative terms is thus of order $B/C^{1/2} = 4/\sqrt{6}$ which is indeed non-negligible and does not depend on Λ . A detailed study of the instanton bag solution using the full DBI+CS action is beyond the scope of this paper. We do not expect, at least in the almost-BPS regime, a qualitative change in the solution.

6 Chiral symmetry restoration

The purpose of this section is to discuss the phenomenon of chiral symmetry restoration at high-density.

Let us first discuss the basic features of chiral symmetry breaking in the SS model with the linear expansion in eigenmodes. The theory lives in the effective geometry (3.1), where the left and right flavour branes correspond to the left and right limits of the holographic coordinate $z \rightarrow \pm\infty$. The YM action in this metric is

$$S = \int d^4x dz \operatorname{tr} \left(-\frac{1}{2H(z)^{1/2}} F_{\mu\nu}^2 - H(z)^{3/2} F_{\mu z}^2 \right). \quad (6.1)$$

We linearly expand around the vacuum state

$$A_\mu = \sum_n B_\mu^n(x_\mu) \psi_n(z) \quad A_z = \sum_n \varphi^n(x_\mu) \phi_n(z), \quad (6.2)$$

We take ϕ_n to be the derivative of ψ_n . The boundary conditions correspond to the vanishing of the sources at the conformal boundaries, which is

$$\psi_n(\pm\infty) = 0 \quad \text{for } n > 0. \quad (6.3)$$

This is the condition that quantizes the mesons states. n odd or even correspond respectively to even or odd states and $n = 0$ is a case to be treated with special care. ψ_n solves the equation

$$H(z)^{1/2} \partial_z (H(z)^{3/2} \partial_z \psi_{(k)}^\pm(z)) + k_n^2 \psi_{(k)}^\pm(z) = 0. \quad (6.4)$$

The action becomes then

$$S = \sum_n (\psi_n, \psi_n) \int d^4x \left(-\frac{1}{4} (\partial_\mu B_\nu^n - \partial_\nu B_\mu^n)^2 + \frac{k_n^2}{2} (B_\mu^n - \partial_\mu \varphi^n)^2 \right), \quad (6.5)$$

and the metric in $\psi(z)$ functional space is

$$(\psi_1, \psi_2) = \int dz H(z)^{-1/2} \psi_1(z) \psi_2(z) \quad (6.6)$$

with ψ_n, ψ_m that are orthogonal if $n \neq m$. For $n \geq 1$ we can eliminate φ 's with a gauge transformation, and the action is then that of a vector boson with mass k_n . When $n = 0$ also $k_0 = 0$, and this gives the action of the pion. This is a special case because the boundary condition (6.3) is not satisfied but nevertheless there is no source at the boundary.

If we expand around another state, we need the particular multi-instanton background which solves the finite density problem. The spectrum in the dual theory always consists in a tower of vector bosons plus the pions.

Vector mesons come in pairs, one vectorial V and one axial A , under the parity symmetry $z \rightarrow -z$. In our conventions, these correspond respectively to the choice of n being odd or even. One of the simplest observables that probes chiral symmetry breaking is the mass splitting between the axial and vectorial states:

$$\eta_m = \frac{M_{2m} - M_{2m-1}}{M_{2m} + M_{2m-1}} \quad (6.7)$$

This test can be performed at every level $m > 0$, although the lower ones give, in general, the biggest η . If η_m is different from zero, chiral symmetry is broken. If η_m is zero, or 'almost' zero, the V and A states are degenerate, and chiral symmetry is restored, or 'almost' restored. In the vacuum, the two left and right branes are connected by the geometry, and chiral symmetry is thus broken. This may not be the case in the presence of something in the middle that could prevent communication between the two sides.

Chiral symmetry is restored, for example, at high temperature in the SS model. Introducing finite temperature leads to competition between the Euclidean time circle τ and the x_5 circle on which to close the topology. This may lead to a phase transition with chiral symmetry restored. In this case, the geometry of space-time has an Hawking-Page phase transition, and the two branes become disconnected by the presence of a horizon. This is a drastic change in the topology, and the V and A states become absolutely degenerate, i.e. η_m is exactly zero for every level m . At finite chemical potential, the situation is more subtle. We will be mainly interested with zero temperature case, so the topology of space-time remain unchanged (3.1). Chiral symmetry restoration can be explained just within the effective action (3.2).

We consider first a toy model that illustrates a simplified version of the phenomenon we want to discuss. This is the quantum mechanical problem of a particle in a double-well potential with Hamiltonian

$$H = -\frac{1}{2} \left(\frac{d}{dx} \right)^2 + \frac{v^2}{2} (x^2 - 1)^2 \quad (6.8)$$

The potential has a parity symmetry $x \rightarrow -x$. In case of a very large potential barrier, $v \gg 1$, we can approximate the eigenstates energies as

$$E_{m,\pm} \simeq \frac{1}{2} + m \mp \mathcal{O}(e^{-4v/3}) \quad \text{for} \quad m \ll v \quad (6.9)$$

with $m \in \mathbb{N}$. These states are localized near the two vacua of the potential and come in pairs. The potential provides a barrier for the states that have energy below its maximum height. For the states below this barrier, we have an approximate degeneracy between V and A states. The splitting between odd and even states can occur only through the tunneling below the barrier, and it is thus suppressed exponentially by the instanton action $e^{-4v/3}$. The situation in HQCD at high-density, as we are going to see, is analogue to this toy model. The instanton charge provides a potential barrier between the left and right boundaries. We then have to determine under which conditions the barrier can seal the two sides from communication with each other, at least for some of the low-energy states, thus providing a mechanism for an effective chiral symmetry restoration. Note that, as for the toy model, the chiral symmetry restoration can never be exact but only up to exponentially small terms. This is expected because, unlike the high temperature case, the left and right branes are always connected by the geometry.

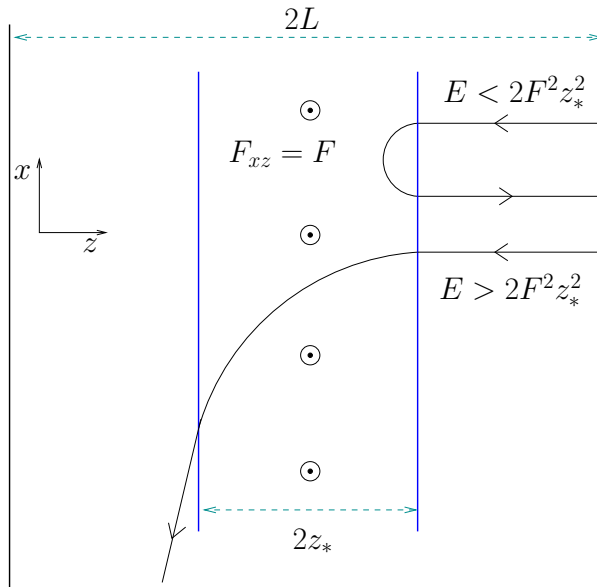


Figure 10: Charged particle tunneling a magnetic field strip.

We now consider a second toy model, which is a step closer to the real thing. We take a charged particle living on a strip $-L < z < L$ and $-\infty < x < \infty$, and coupled to a background gauge field. The equation of motion is the following covariant version of the Klein-Gordon equation

$$\left(\frac{1}{2}(\partial_t - iA_t)^2 - \frac{1}{2}(\partial_x - iA_x)^2 - \frac{1}{2}(\partial_z - iA_z)^2 \right) \psi(t, x, z) = 0. \quad (6.10)$$

In a static background we can solve the eigenvalues equation

$$\left(-\frac{1}{2}(\partial_x - iA_x)^2 - \frac{1}{2}(\partial_z - iA_z)^2 \right) \psi_n(x, z) = \epsilon_n \psi_n(x, z). \quad (6.11)$$

This is the same of the Schrodinger equation for of a non-relativistic quantum particle with mass/ $\hbar^2 = 1$. This analogy may be useful. For states which do not have momentum in the x direction, the eigenvalues λ_n are related to the mass in the holographic interpretation, precisely

$$\epsilon_n = \frac{M_n^2}{2} \quad \text{for } k_x = 0 \quad (6.12)$$

In the vacuum $A_{x,z} = 0$, the spectrum of the operator (6.11) is $\epsilon_n = (1+n)^2/L$, where n being odd or even corresponds to the parity with respect to $z \rightarrow -z$ and clearly there is no degeneracy between V and A states. We then turn on a constant magnetic field $F_{xz} = F$ in a smaller strip $-z_* < z < z_*$ with $z_* < L$. The phenomenon of magnetic trapping is quite clear by considering the classical particle trajectories in Figure 10. This in the sense of the non-relativistic analogy mentioned before. For a particle to be able to cross the magnetic strip, the radius of the trajectory in the constant magnetic field zone $\sqrt{2\epsilon}/F$ must be at least equal to the strip size $2z_*$. There is an effective energy barrier $\simeq (Fz_*)^2$ between the left and right regions. The left and right states, if confined in the regions without the magnetic field, have energies

$$\epsilon_{m;V,A} = \frac{\pi^2(1+m)^2}{2(L-z_*)^2} \mp \mathcal{O}\left(e^{-\alpha Fz_*^2}\right) \quad (6.13)$$

with $m \in \mathbb{N}$:

$$l_p \simeq \frac{1+m}{(L-z_*)F} . \quad (6.14)$$

The condition to have V and A degeneracy is $l_p \ll z_*$, which, for the lowest state $m = 0$, is

$$\frac{1}{(L-z_*)F} \ll z_* . \quad (6.15)$$

To be more explicit, we take the following gauge to reproduce the desired magnetic field

$$\begin{aligned} A_x &= 0 & z_* \geq z \geq L \\ A_x &= F(z - z_*) & -z_* \leq z \leq z_* \\ A_x &= -2Fz_* & -L \geq z \leq -z_* \end{aligned} \quad (6.16)$$

with $A_t = A_z = 0$. The eigenstates can be written as

$$\psi(t, x, z) = e^{ik_t t - ik_x x} \psi_n(z) , \quad (6.17)$$

where $k_t^2 - k_x^2 = M_n^2$ is the mass square from the x, t perspective. With this ansatz, the eigenvalue equation becomes

$$-\frac{1}{2}\psi_n(z)'' + \frac{(F(z - z_*) - k_x)^2}{2}\psi_n(z) = \frac{M_n^2}{2}\psi_n(z) , \quad (6.18)$$

which is the analogue of (6.4). The wave function $\psi_n(z)$ is exponentially damped in the magnetic field region. This damping is smaller if we increase the particle mass M_n and/or if we give a momentum in the x direction, as is also clear from Figure 10. For the low-energy states, the penetration length is given by formula (6.14).

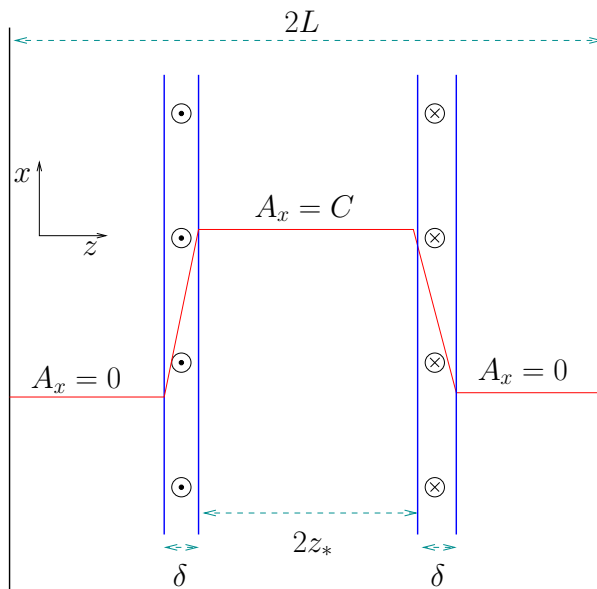


Figure 11: Charged particle tunneling a ‘pure gauge’ strip.

We now consider a third toy model (Figure 11), which contains yet a different effect that will have to be considered when we will deal with the real thing. We take the same charged particle as before living on a strip $-L < z < L$ and $-\infty < x < \infty$, and coupled to a background gauge field. We then turn on a pure gauge field $A_x = C$ with C a constant in a smaller strip $-z_* < z < z_*$ with $z_* < L$:

$$\begin{aligned}
 A_x = 0 & & z_* + \delta \geq z \geq L \\
 A_x = C & & -z_* \leq z \leq z_* \\
 A_x = 0 & & -L \geq z \geq -z_* - \delta
 \end{aligned} \tag{6.19}$$

with $A_t = A_z = 0$. The two walls at the edges of the strip have thickness $\delta \ll z_*$. Here a magnetic field F_{xz} is inevitably turned on to have the matching of the gauge field. We assume that this happens in the simplest way, a linear function homogeneous in x . So the magnetic field inside the two walls is respectively $F_{xz} = \pm C/\delta$.

There is now a massless eigenstate that can propagate inside the strip since it is a pure gauge. The only difference is that this state must have a phase changing in the x direction to cancel the constant field e^{iCx} . So the main source of tunneling between the left and right side, takes place inside the two walls of thickness δ ,

and is just given by the overlap between the massless states inside and outside the strip. The penetration length now given by

$$l_p \simeq \frac{(1+m)\delta}{(L-z_*)C} \quad (6.20)$$

The condition to have V and A degeneracy is $l_p \ll \delta$, that, for the lowest state $m = 0$, is

$$\frac{1}{(L-z_*)C} \ll 1. \quad (6.21)$$

Note that δ disappears from this condition.

Now we finally consider the real problem of HQCD in the instanton bag background. The problem is quite complex, and we cannot provide an analytic solution for the wave functions and the spectra as in the vacuum state (6.4). We have to rely on analogies with the previous toy models. There are two different sources of tunneling we need to consider, one is mimicked by second toy model of Figure 10, the other by the third toy model of Figure 11.

The theory is defined on the metric (3.1), which is effectively a box with finite size, and this is what provides the quantization of the vector mesons' masses. The analogy with the previous two toy models is that the size of the strip L is the curvature scale.

We begin from the almost-BPS limit, which is valid in the region of densities $\Lambda^{3/2} \ll Q \ll \Lambda^2$. The $\Lambda^{3/2}$ lower bound is when the instantons begin to populate the holographic direction, and it also coincides with the microscopic wall structure, $l \simeq \delta \simeq 1/\sqrt{\Lambda}$, being smaller than the distance between the two walls, which is of order Q/Λ^2 . The upper bound coincides with the wall position being much smaller than the curvature scale $z_w \simeq Q/\Lambda^2 \ll 1$. In this case, the wave length of the particle confined in the empty sides is of order one (this is the analogue of $1/(L-z_*)$ in the toy model).

The first effect to consider is the tunneling as in Figure 10. Between the two walls the fields are

$$F_{12} = F_{3z} = BU(x_1, x_2)t_{\text{su}(2)}U(x_1, x_2)^{-1} \quad (6.22)$$

A gauge transformation $U(x_1, x_2)$ is necessary, as we discussed in Section 2, for the gauge fields not to have Dirac string singularities at the both boundaries. The magnetic fields oscillate in all the $\text{su}(2)$ generators. The vector boson state are instead waves coming from the empty sides in a fixed generator of the $\text{su}(2)$ algebra.

The F field of the toy model in Figure 10 is the analogue of this F_{zx_3} field. We will neglect the magnetic field F_{12} for simplicity. First, we check if the oscillations of the magnetic field generator, are fast enough respect to be momentum of the wave hitting the monopole wall from the empty side. This is indeed the case because the momentum of the waves confined in the empty regions is or order one

while the momentum of the monopole wall lattice is $1/l \simeq 1/\sqrt{\Lambda}$. The the vector bosons states do not have enough energy to resolve the microscopic structure of the wall, neither to see the fluctuations of the magnetic fields (6.22). Then we have to check if the size of the magnetic strip is large enough to separate the left and right sides. The penetration length is of order $1/F \simeq 1/\Lambda$ and is much smaller than the wall's distance $z_w \simeq Q/\Lambda^2$ in this regime. Therefore, the two sides are indeed separated by a potential barrier, at least for the channel described by Figure 10.

There is yet another possible source of tunneling. The monopole wall solution is essentially an Abelian solution far from the wall. In the Dirac gauge, the fields are all directed in one particular direction in the algebra $\mathfrak{su}(2)$, see (2.3), (2.4). So the states of the vector boson fields which are directed in the same direction are completely transparent to the magnetic fields and they pass through the region between the two walls as free fields. The hedgehog gauge does not make this massless states disappear, they just have particular winding in the x_1 and x_2 direction to compensate for the gauge transformation. This is exact analogue to what happens in the toy model of Figure 11. The condition for having a barrier is that the wave length of the particle confined in the empty sides must be much smaller that the microscopic wave length $1/l$, and this we already checked to be the case.

We then go to the high-density limit $Q \gg \Lambda^2$, and we have to compute the equivalent of the energy scale (6.13) in the toy model. For this, is convenient to go first in the η coordinate where the metric is conformally flat, which for $z \gg 1$ and $\eta \ll 1$ is

$$ds^2 = z(\eta)^{4/3} (dx_\mu dx^\mu + d\eta^2) \quad z(\eta) \simeq \frac{27}{\eta^3} . \quad (6.23)$$

The typical momentum of a particle confined in the empty region $z > z_w$, in these coordinate, is

$$k_\eta \simeq \frac{1}{\eta_w} \simeq \frac{3}{z_w^{1/3}} . \quad (6.24)$$

We then use the coordinate transformations to go in the \tilde{x}, \tilde{z} coordinates, the ones in which the metric is (4.29) near the wall. The result is

$$k_{\tilde{z}} \simeq \frac{k_\eta}{z_w^{2/3}} \simeq \frac{3}{z_w} . \quad (6.25)$$

This is the momentum of the wave hitting the monopole wall in a locally Minkowski frame.

The next step is to compare this with the lattice size of the monopole wall. The following inequalities

$$k_{\tilde{z}} \ll \frac{1}{\tilde{l}} \quad \implies \quad \Lambda^{1/2} \ll Q^{1/2} \quad (6.26)$$

mean that the momentum $k_{\bar{z}}$ is never large enough to see the microscopic structure of the wall so we can average out the fluctuations of the magnetic field. Then we want to estimate the penetration length of the wave with momentum (6.25) when it enters the magnetic field region. The penetration length is from the equation

$$l_p \simeq \frac{k_{\bar{z}}}{F_{3\bar{z}}} \propto \frac{1}{Q^{2/5} \Lambda^{1/5}}, \quad (6.27)$$

which is even smaller than the wall thickness δ . Thus, the two sides are not communicating also in the $Q \gg \Lambda^2$ limit.

Being the chiral symmetry restoration only up to exponentially small terms, the V - A mass splitting is never exactly zero, and in particular the pion, as a massless state in the spectrum of the theory, is always present. The pion wave function $\phi_0(z)$ is approximately constant in the two empty sides of the instanton bag, with opposite sign, and joined by an exponentially suppressed tail in the middle. This implies that the higher derivative interactions between pions and between pion and the massive vector bosons is exponentially suppressed. It would be interesting to understand between this aspect in terms of the chiral condensate as in [34, 35] and the chiral wave. The computation in the instanton bag background is not yet exact. A precise computation would require the knowledge of the internal structure of the walls.

7 Conclusions

In the first part of the paper, we discussed a multi-instanton solution in flat space which is periodic in three directions and finite in the fourth direction. We called this an instanton bag because, in some opportune limit, it can be described by an homogeneous distribution of self-dual fields trapped between a monopole wall and a Kaluza-Klein monopole wall. We embedded the instanton bag in the Sakai-Sugimoto model. This is the dual of a phase of high-density baryons in the QCD-like theory defined on the boundary. The parameters of the solutions have been determined by the constrained energy minimization, have been analytically solved in two limits of intermediate and large densities, and have been confronted with the numerical solution.

A transition from a lattice of instantons and a lattice of monopoles and KK monopoles pairs has been discussed in [11] under the name of ‘dyonic salt’. Our construction is somehow an extension of this because we show, using the monopole walls, how to extend this to higher densities where the holographic direction is also probed. The fact that at high densities the instantons start to probe the holographic direction has been discussed [7, 9, 10] and linked to the existence of a quarkionic phase. We showed that that a configuration similar to the dyonic salt can be extended to arbitrary high densities and probe the holographic direction.

We still cannot perform the minimization over all the possible multi-instanton moduli space. The instanton bag configuration we considered in this paper, is just

one particular case, for we can compute the fields, the energy, and then minimize the moduli.

This instanton bag phase is intrinsically non-dilute, i.e. the individual instantons components cannot be distinguished and are larger than their average separation. Previous results in the toy model [1] and also the qualitative analysis of Section 3 showed that non-dilution is an inevitable feature of large density solutions and becomes applicable exactly when the solitons start to populate the holographic direction.

The restoration of chiral symmetry is related to the non-dilution of this phase. The non-Abelian field strength is continuously spread in the bulk, as opposed to a dilute phase in which it is confined to the instanton cores. This considerably affects the equation of motion for the gauge fields in the bulk, and thus creates a barrier between the left and right branes leading to an effective chiral symmetry restoration.

Acknowledgments

I thank D. Tong, M. Blake and K. Wong for discussions and collaboration to the initial stage of this project. I thank P. Sutcliffe for discussions, in particular during the closely related projects [1, 27]. This work was partially funded by the EPSRC grant EP/K003453/1 and now by the grant ‘Rientro dei Cervelli, RLM’ of the Italian government.

References

- [1] S. Bolognesi and P. Sutcliffe, “A low-dimensional analogue of holographic baryons,” arXiv:1311.2685 [hep-th].
- [2] S. Bolognesi, “Multi-monopoles and magnetic bags,” Nucl. Phys. B **752** (2006) 93 [hep-th/0512133].
- [3] P. Sutcliffe, “Hyperbolic vortices with large magnetic flux,” Phys. Rev. D **85** (2012) 125015 [arXiv:1204.0400 [hep-th]].
- [4] D. Harland, S. Palmer and C. Saemann, “Magnetic Domains,” arXiv:1204.6685 [hep-th].
- [5] D. V. Deryagin, D. Y. Grigoriev and V. A. Rubakov, “Standing wave ground state in high-density, zero temperature QCD at large $N(c)$,” Int. J. Mod. Phys. A **7** (1992) 659.
- [6] E. Shyster and D. T. Son, “On finite density QCD at large $N(c)$,” Nucl. Phys. B **573** (2000) 434 [hep-ph/9905448].

- [7] J. de Boer, B. D. Chowdhury, M. P. Heller and J. Jankowski, “Towards a holographic realization of the Quarkyonic phase,” arXiv:1209.5915 [hep-th].
- [8] L. McLerran and R. D. Pisarski, “Phases of cold, dense quarks at large $N(c)$,” Nucl. Phys. A **796** (2007) 83 [arXiv:0706.2191 [hep-ph]].
- [9] V. Kaplunovsky, D. Melnikov and J. Sonnenschein, “Baryonic Popcorn,” arXiv:1201.1331 [hep-th].
- [10] V. Kaplunovsky and J. Sonnenschein, “Dimension Changing Phase Transitions in Instanton Crystals,” arXiv:1304.7540 [hep-th].
- [11] M. Rho, S. -J. Sin and I. Zahed, “Dense QCD: A Holographic Dyonic Salt,” Phys. Lett. B **689** (2010) 23 [arXiv:0910.3774 [hep-th]].
- [12] Y. -L. Ma, M. Harada, H. K. Lee, Y. Oh, B. -Y. Park and M. Rho, “Dense baryonic matter in the hidden local symmetry approach: Half-skyrmions and nucleon mass,” Phys. Rev. D **88** (2013) 1, 014016 [arXiv:1304.5638 [hep-ph]].
- [13] M. Rozali, H. -H. Shieh, M. Van Raamsdonk and J. Wu, “Cold Nuclear Matter In HQCD,” JHEP **0801** (2008) 053 [arXiv:0708.1322 [hep-th]].
- [14] K. -M. Lee, “Sheets of BPS monopoles and instantons with arbitrary simple gauge group,” Phys. Lett. B **445** (1999) 387 [hep-th/9810110].
- [15] R. S. Ward, “A Monopole Wall,” Phys. Rev. D **75** (2007) 021701 [hep-th/0612047].
- [16] S. Bolognesi and D. Tong, “Monopoles and Holography,” JHEP **1101** (2011) 153 [arXiv:1010.4178 [hep-th]].
- [17] S. A. Cherkis and R. S. Ward, “Moduli of Monopole Walls and Amoebas,” JHEP **1205** (2012) 090 [arXiv:1202.1294 [hep-th]].
- [18] M. Hamanaka, H. Kanno and D. Muranaka, “Hyperkahler Metrics from Monopole Walls,” Phys. Rev. D **89** (2014) 065033 [arXiv:1311.7143 [hep-th]].
- [19] S. A. Cherkis, “Phases of Five-dimensional Theories, Monopole Walls, and Melting Crystals,” arXiv:1402.7117 [hep-th].
- [20] R. Maldonado and R. S. Ward, “Dynamics of monopole walls,” arXiv:1405.4646 [hep-th].
- [21] K. -M. Lee and P. Yi, “Monopoles and instantons on partially compactified D-branes,” Phys. Rev. D **56** (1997) 3711 [hep-th/9702107].
- [22] K. -M. Lee and C. -h. Lu, “SU(2) calorons and magnetic monopoles,” Phys. Rev. D **58** (1998) 025011 [hep-th/9802108].

- [23] T. C. Kraan and P. van Baal, “Periodic instantons with nontrivial holonomy,” Nucl. Phys. B **533** (1998) 627 [hep-th/9805168].
- [24] Kimyeong Lee, *private communication*, March 2011
- [25] D. K. Hong, M. Rho, H. -U. Yee and P. Yi, “Chiral Dynamics of Baryons from String Theory,” Phys. Rev. D **76** (2007) 061901 [hep-th/0701276 [HEP-TH]].
- [26] H. Hata, T. Sakai, S. Sugimoto and S. Yamato, “Baryons from instantons in HQCD,” Prog. Theor. Phys. **117** (2007) 1157 [hep-th/0701280 [HEP-TH]].
- [27] S. Bolognesi and P. Sutcliffe, “The Sakai-Sugimoto soliton,” arXiv:1309.1396 [hep-th].
- [28] Y. Kim, S. Lee and P. Yi, “Holographic Deuteron and Nucleon-Nucleon Potential,” JHEP **0904** (2009) 086 [arXiv:0902.4048 [hep-th]].
- [29] K. Ghoroku, K. Kubo, M. Tachibana, T. Taminato and F. Toyoda, “Holographic cold nuclear matter as dilute instanton gas,” arXiv:1211.2499 [hep-th].
- [30] C. Ford, J. M. Pawłowski, T. Tok and A. Wipf, “ADHM construction of instantons on the Torus,” Nucl. Phys. B **596** (2001) 387 [hep-th/0005221].
- [31] T. Sakai and S. Sugimoto, “Low energy hadron physics in HQCD,” Prog. Theor. Phys. **113** (2005) 843 [hep-th/0412141].
- [32] E. Witten, “Anti-de Sitter space, thermal phase transition, and confinement in gauge theories,” Adv. Theor. Math. Phys. **2** (1998) 505 [hep-th/9803131].
- [33] V. Kaplunovsky and J. Sonnenschein, “Searching for an Attractive Force in Holographic Nuclear Physics,” JHEP **1105** (2011) 058 [arXiv:1003.2621 [hep-th]].
- [34] O. Aharony and D. Kutasov, “Holographic Duals of Long Open Strings,” Phys. Rev. D **78** (2008) 026005 [arXiv:0803.3547 [hep-th]].
- [35] S. Seki and S. -J. Sin, “Chiral Condensate in HQCD with Baryon Density,” JHEP **1208** (2012) 009 [arXiv:1206.5897 [hep-th]].